Optimum MASW Survey — Revisit after a Decade of Use

Choon B. Park[1] and Mario Carnevale[2]

[1]ParkSeismic LLC, 2 Balsam Cir, Shelton, CT 06484; PH (347) 860-1223; email: choon@parkseismic.com
[2]Hager GeoScience, Inc., 596 Main Street, Woburn, MA 01801; PH (781) 935-8111; email: ihagerg1350@earthlink.net

ABSTRACT

As an attempt to study systematically on the optimum source offset—the distance between source and the closest receiver—and total receiver spread length with the MASW method, we present our observations with modeling and field data sets indicating that the most accurate analysis of phase velocities can be accomplished only for wavelengths up to one spread length, and subsequent analysis for the longer wavelengths inevitably involves a certain degree of fluctuating inaccuracy that seems to originate from the Gibbs' phenomenon of Fourier transformation. The inaccuracy, however, seems to be within five percent for those wavelengths shorter than twice the spread length. Also, results from the field data study suggest that importance of the source offset has been previously underestimated and the maximum wavelength can be extended simply by extending the source offset. In addition, they showed that phase velocities tend to be underestimated if the source offset is smaller than one spread length. The degree of underestimation, however, appears highly site dependent and sometimes becomes negligible even if the source offset is as short as only one receiver spacing.

INTRODUCTION

Since its first introduction in the late 90s, the multichannel analysis of surface wave (MASW) method (Park et al., 1999) has been extensively used and researched for various projects and topics. In consequence, it has been continuously evolving in its field and data-processing strategies. As it was then based on observations made through a limited number of field tests, some recommendations in optimum field parameters made in early publications often have been under debate among practitioners and investigators as some contradicting observations were made. Among them are the optimum distance between the source and the nearest receiver, commonly referred to source offset (X1), and the receiver spread length (L) (Park et al., 1999; Zhang et al., 2004; Ryden and Mooney, 2009; Yoon and Rix, 2009).

The importance of source offset (X1) was related to the observation that, within a certain distance from the source, propagation properties of surface waves are different from those at further distances away and therefore subsequent measurement should avoid this field near the source point (Richart et al., 1970; Gucunski and Woods, 1991; Stokoe et al., 1994). With the exact mechanism not fully understood, although commonly considered a multi-factored phenomenon, this effect has been

frequently claimed to be responsible for many confusing observations under the name of "near-field" effect. Attributing factors commonly studied include (Ryden and Mooney, 2009): (1) non-planar propagation of surface waves due to cylindrical spreading, (2) surface waves not reaching maximum energy level yet due to some inherent properties in wave generation, (3) interference with relatively strong body waves, and (4) strain-dependent nonlinear seismic velocity due to the excessive strain level. The most common influence of the near field effect on the surface wave analysis is the phase velocities being different from (usually lower than) those observed elsewhere free of this effect.

The importance of receiver spread length (L), on the other hand, was unrelated to any field phenomena but originated solely from the data processing perspective that the maximum wavelength measurable (λmax) increases with the receiver spread length and so does the maximum investigation depth (Zmax), which has been usually considered to be a fraction of λmax (Rix and Leipski, 1991; Stokoe et al., 1994). It has been normally considered that $\lambda max \approx L$. In consequence, Zmax usually has been considered to be a fraction of L (e.g., $Zmax \approx 0.5L$), based on the notion that the inversion process can resolve seismic velocities as deep as a certain fraction of λmax (e.g., $0.5\lambda max$).

It has been frequently observed during MASW field testing that the lowest limit of the analyzable frequency could be lowered simply by increasing the source offset (X1) alone without extending the spread length (L), raising a speculation that the influence of this particular field parameter on the effective surface wave generation might be originally underestimated (Park and Shawver, 2009). For example, the imaged dispersion trend would be extended to those wavelengths longer than the spread length (i.e., $\lambda max \geq L$) when source offset was longer than the previously recommended value of one half of the spread length (i.e., $X1 = L/2$). In this sense, it has been speculated that Zmax can be increased as well simply by increasing X1 alone without extending the spread length that may result in a reduced lateral resolution. Validity of analyzed phase velocities in this range of wavelength longer than spread length (i.e. $\lambda \geq L$), however, has been under question. In addition, a greater variation in dispersion trend was often observed from one field record to another at frequencies near this low end than at the higher frequencies although these records were acquired at similar locations, raising a speculation that the variation might not be real.

On the other hand, a source offset significantly smaller than spread length (for example, $X1 = L/4$) was often used during normal MASW surveys with an assertion that the distance disturbed by the near field effect should be smaller than the one usually recommended by the traditional SASW method (for example, $X1 \geq L/2$) (Park et al., 1999). This criterion was based on the limited MASW field testing at the time, and also on the notion that multichannel plane-wave processing should filter out any adverse influence, if it exists. We test validity of this criterion based on observations with field data sets from different areas.

RECEIVER SPREAD LENGTH (L)

Although, in theory, the maximum wavelength (λmax) that can be analyzed should not depend on the length of receiver spread length (L) and be infinite if no

uncertainties are introduced in the field measurement, in reality λmax depends on L because of the uncertainties (noise) always included in the measurement. Therefore, the number of repeated measurements within a given spread length increases as wavelength becomes shorter and this results in the possibility of an increased accuracy in analysis through various types of signal-enhancing techniques. Based on mostly empirical observations, λmax was usually considered to be about twice the receiver separation (d) in the traditional two-receiver approach of the Spectral Analysis of Surface Waves (SASW) method (Stokoe et al., 1994), whereas it was not clearly studied with the MASW approach. Taking this empirical SASW criterion into consideration, MASW adopted a similar concept that λmax is twice as long as the receiver spread length (L); i.e., λmax = 2L. Then, the maximum investigation depth (Zmax) of the MASW method was considered equal to about one-half of λmax; i.e., Zmax = λmax/2 = L. Results from many field tests, however, indicated that this was overestimated and a more practical criterion should be Zmax = L/2, which is most commonly adopted nowadays as an empirical criterion.

To study the dependence of λmax on L (therefore Zmax on L) with the MASW approach, synthetic multichannel records were created in which surface waves propagating at a constant phase velocity of 500 m/sec in the frequency band of 1-2-100-150 Hz (Figure 1a) were modeled according to the algorithm by Park and Miller (2005b). Here, terms for attenuation by material damping and divergence by cylindrical spreading were not included in order to eliminate unrelated issues that may have obscured phenomena being studied. The modeled field record in Figure 1b

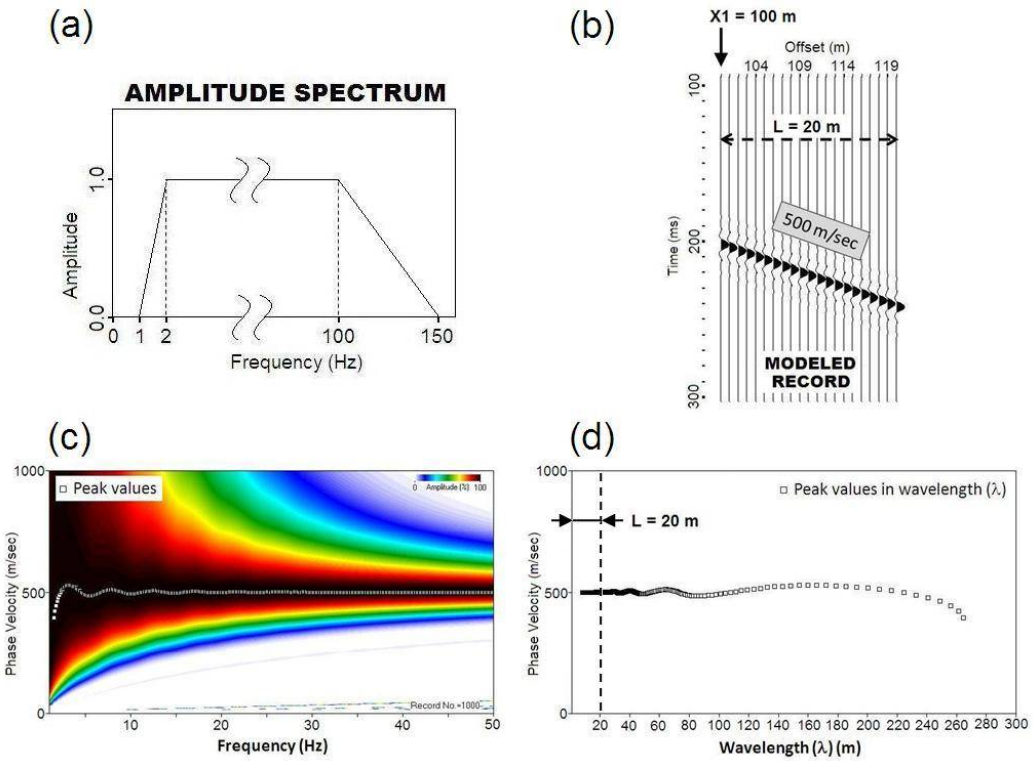

Figure 1. (a) Amplitude spectrum used to model (b) a field record. Its (c) dispersion image with extracted curve marked and its display in (d) wavelength.

therefore contains simply waves occurring at different arrival times at different offsets and nothing else.

Figure 1c shows the dispersion image of the synthetic record in Figure 1b constructed by using the most commonly used 2D wavefield transformation method from Park et al. (1998). A dispersion curve was extracted by following energy maxima (peaks) approximately in the 2-50 Hz range in the image and displayed in Figures 1c and 1d in frequency and wavelength, respectively. It is noted the exact value of 500 m/sec was recovered for wavelengths approximately smaller than one spread length ($\lambda \leq L$), whereas it starts to deviate for longer wavelengths.

Similar experiments were performed with synthetic records of two different spread lengths of L = 20 m and L = 40 m, respectively, and ten different source offsets (X1's). Results are shown in Figure 2. It can be noticed phase velocities start to deviate once wavelength exceeds L (i.e., $\lambda \geq L$) and the way it deviates changes with X1 as well as L. The deviation appears to oscillate at first very slowly when X1 is small (e.g., $X1 \leq L$) and then more rapidly as X1 increases. Overall magnitude of the oscillation gradually increases with X1 until X1 reaches a certain ratio and then decreases before it starts to increase again, a pattern of another oscillation. For example, the magnitude increases until X1 becomes 4L when L = 20 m, and then decreases gradually until it becomes almost negligible at X1 = 8L. On the other hand, with L = 40 m the magnitude of oscillation reaches its first peak at X1 = 2L, becomes negligible at X1 = 4L, reaches its second peak at X1 = 6L, and becomes negligible again at X1 = 8L. The magnitude of these peaks themselves appears to gradually attenuate as X1 increases. This periodic behavior in deviation pattern seems to originate from the inherent property of Gibbs' phenomenon with Fourier transformation (Oppenheim and Schafer, 1989). The implication of this phenomenon is that the truncated Fourier series approximation of a function with abruptly changing points exhibit ripples (overshoots and undershoots) near these points. Similar situations may exist during the 2-D wavefield transformation of dispersion imaging at those wavelengths exceeding receiver spread length and also for those lower frequencies where surface wave energy drops abruptly. Examination of all curves shown in Figure 2 indicates that maximum error in phase velocity caused by this deviation is less than five percent (5%) for wavelengths of $L \leq \lambda \leq 2L$, regardless of X1 used. A similar oscillation feature in dispersion curves is observed with field data sets as described in next section.

SOURCE OFFSET (X1)

The importance of optimum X1 is to minimize adverse influence from the near-field effect. It has been known the minimum distance (d_c) to avoid adverse influence from near-field effects is dependent on wavelength (λ) and increases in proportion; $d_c = k\lambda$. Although the ratio (k) between d_c and λ has been reported slightly different from different studies with the SASW method, it has been usually considered to be approximately equal to a half wavelength; $d_c = \lambda/2$ (Gucunski and Woods, 1991; Stokoe et al., 1994). The MASW method adopted the same criterion and therefore an optimum source offset of one-half of the spread length (i.e., X1 = L/2) has been commonly recommended assuming $\lambda max \approx L$. This issue, however, has not been studied sufficiently with MASW to present a clear understanding of the

background mechanism and objective guideline for field operations. We present our results from tests with field data sets. Most recently, from studies with surface waves generated from light weight deflectometer (LWD) and numerical modeling, Ryden and Mooney (2009) reported that a distance of one wavelength is required between the receiver spread center and the source point to be free of near-field effect. This concept conforms to the common practice with MASW that X1 ≥ L/2 with λmax ≈ L.

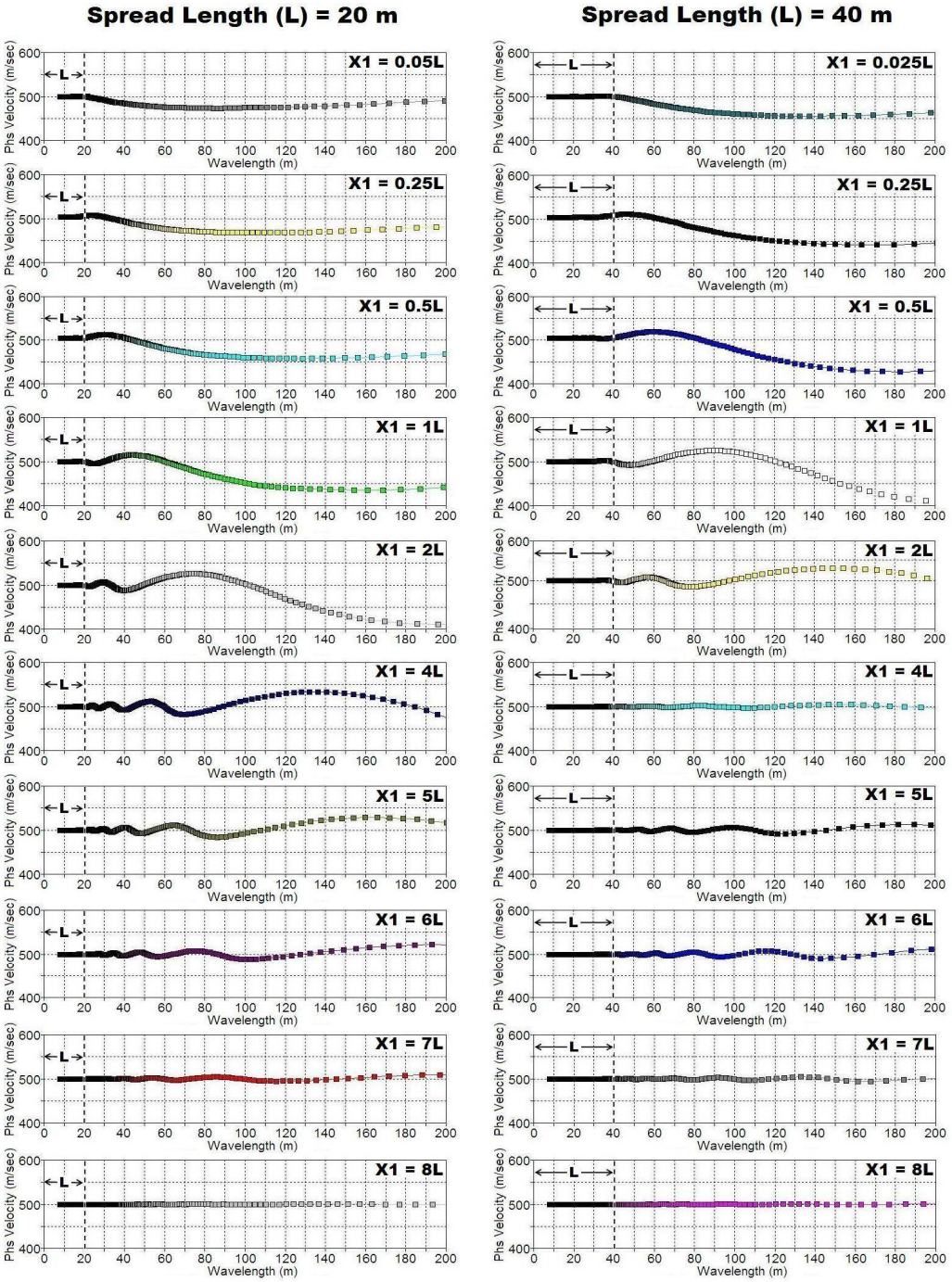

Figure 2. Dispersion curves from synthetic records with receiver spread lengths (L) of 20 m (left) and 40 m (right) for different source offsets (X1's).

Field Data Test

Field data sets (Miller et al., 2003) recorded with a 240-channel acquisition system during the geophysical characterization study at the Smart Weapons Test Range (SWTR) within the Yuma Proving Ground (YPG), Arizona, were used to study the influence of X1 on MASW dispersion analysis (Figure 3). A rubberband aided weight drop (RAWD) seismic source was used to generate surface waves at different locations along a linear 240-channel receiver spread fixed at the same surface location during the survey (Figure 4). The receiver spread consisted of 4.5-Hz geophones with 1-m receiver spacing (dx).

Two zones near the center of the receiver spread were chosen for this study where data sets equivalent of 24-channel and 48-channel recording were prepared that had different source offsets (X1's) (Figure 4). A reference field data set was also prepared by selecting a zone at the center equivalent of 120-channel recording that had different source offsets of X1 = 1dx, 120dx, and 240dx. They were then processed individually to generate dispersion image data sets, which were then stacked together to enhance the overall quality of the image with an increased bandwidth and minimized adverse influence from the near-field effect (Park and Shawver, 2009). A dispersion curve was then extracted from this stacked image by following amplitude peaks in the most prominent energy trend interpreted as fundamental mode (M0). When plotted in wavelength, it had a range of approximately 10-150 m (λmax = 150 m). This curve was then used as a reference curve for the subsequent studies that used records equivalent of much shorter spread lengths of 24 m and 48 m, respectively, because the curve was considered free of any disturbing influence, at least for the wavelength range (e.g., 10-120 m) with which other dispersion curves being studied were compared.

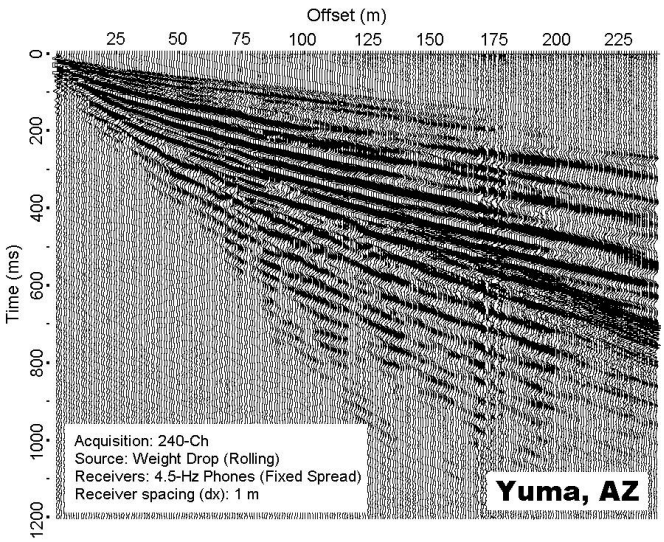

Figure 3. One example of 240-channel field records collected during the project at SWTR near Yuma, AZ (Miller et al., 2003).

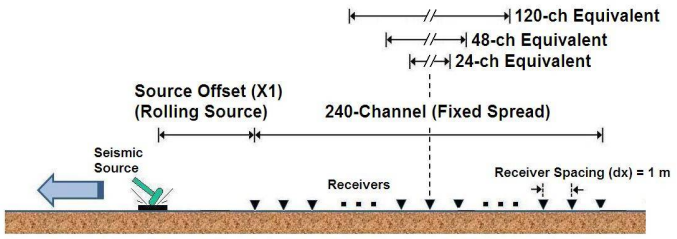

Figure 4. A schematic illustration of field layouts corresponding to subsets of field data prepared for this study.

Source Offset (X1) and Phase Velocity Change

Dispersion curves were extracted from dispersion images processed from ten (10) and six (6) field records of different source offsets (X1's) that were of equivalent 24-channel and 48-channel recording, respectively, centered at the same surface location (Figure 4). These curves are plotted against the reference curve and shown in Figure 5. Fluctuation can be observed with most curves for those wavelengths exceeding one spread length ($\lambda \geq L$) in both cases, conforming to the previous results from experiments with synthetic data sets that appear to originate from the Gibbs' phenomenon (Figure 2). Dispersion curves for the smallest X1 of 1 meter in both cases, however, do not appear to fluctuate in the same manner as others do within the tested range of wavelength, also conforming to the synthetic results. The magnitude of fluctuation in wavelengths in the range of L-2L seems to be less than five percent (5%) if $X1 \geq L$, and that conforms to the synthetic results as well, whereas it becomes greater when $X1 \leq L$, perhaps due to the additional near-field effect explained below. Contrary to the synthetic case, however, the oscillating feature of dispersion curves start even at $\lambda \leq L$ and it is most conspicuous at L = 47 m. This indicates there can be other factor(s) involved in this phenomenon than the Gibbs' property of Fourier transformation previously mentioned.

It can also be seen that phase velocities are underestimated for $\lambda \leq L$ in those cases of $X1 \leq L$. This effect was further tested with more field records equivalent to 48-channel recording with X1's shorter than or comparable to L, and results are shown in Figure 6. The underestimation seems to start once the wavelength becomes longer than half the distance sum of L and X1; i.e., when $\lambda \geq (L + X1)/2$. This also means that it occurs

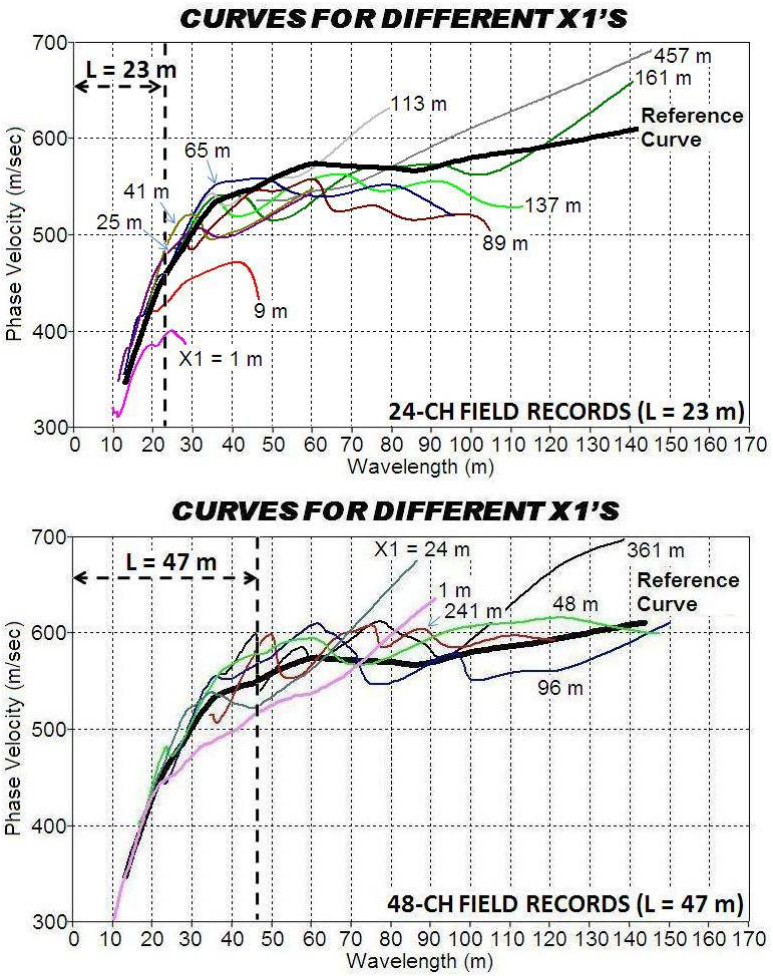

Figure 5. Dispersion curves processed from SWTR field records equivalent of 24- (upper) and 48-channel (lower) recording with different source offsets (X1's).

for those wavelengths longer than half the distance between source and furthest receiver. Apparent overestimation occurs at $\lambda \leq L$ for X1's comparable to L (X1 = 41 m and 49 m) without any obvious reason (perhaps due to ambient noise).

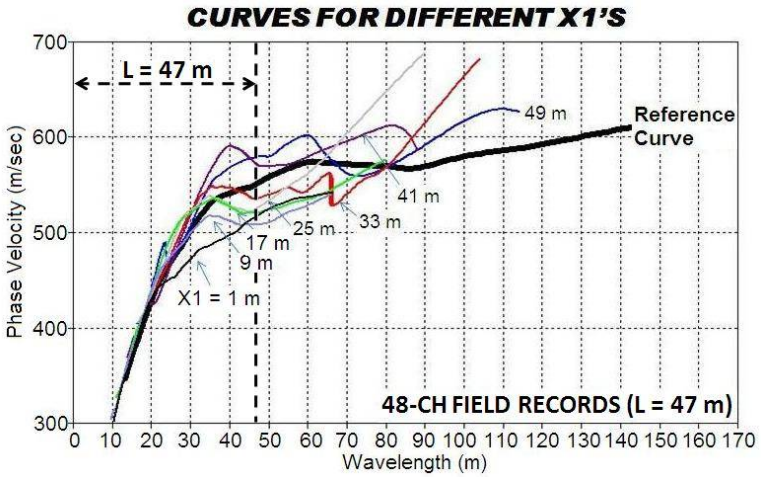

Figure 6. Dispersion curves processed from SWTR field records equivalent of 48-channel recording with source offsets smaller than or comparable to L.

The underestimation, however, appears highly site dependent as shown in Figure 7 from another set of field data collected at the Blue Canyon Wind Farm (Park and Miller, 2005b). Twenty-four field records acquired with a fixed 24-channel receiver spread at two different turbine sites were processed that had all different source offsets ranging from X1 = 1dx to X1 = 24dx. Processed dispersion curves in Figure 7 show the overestimation is minimal or negligible.

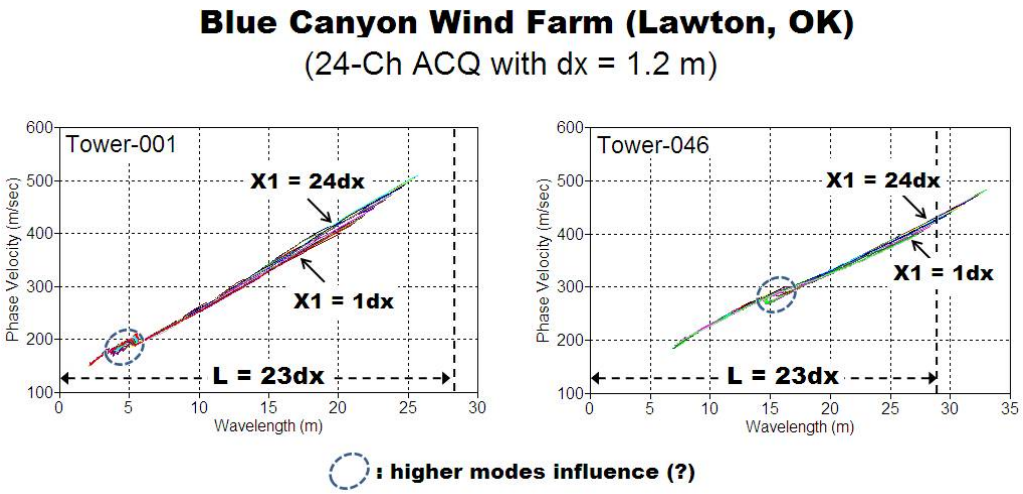

Figure 7. Dispersion curves processed from two sets of field records at two proposed tower sites in Blue Canyon Wind Farm near Lawton, OK. All records were equivalent of 24-channel recording of 1.2 m receiver spacing (dx) with different source offsets of 1dx – 24dx.

Source Offset (X1) and Surface Wave Energy

To illustrate the influence of source offset (X1) on the energy level of lowest frequency surface waves generated, field records equivalent of 120-channel recording were prepared for source offsets of X1 = 12 m, 60 m, 180 m, and 300 m from the SWTR data sets previously used. Figure 8 shows dispersion images processed from each record where the lowest analyzable frequency was marked along with corre-

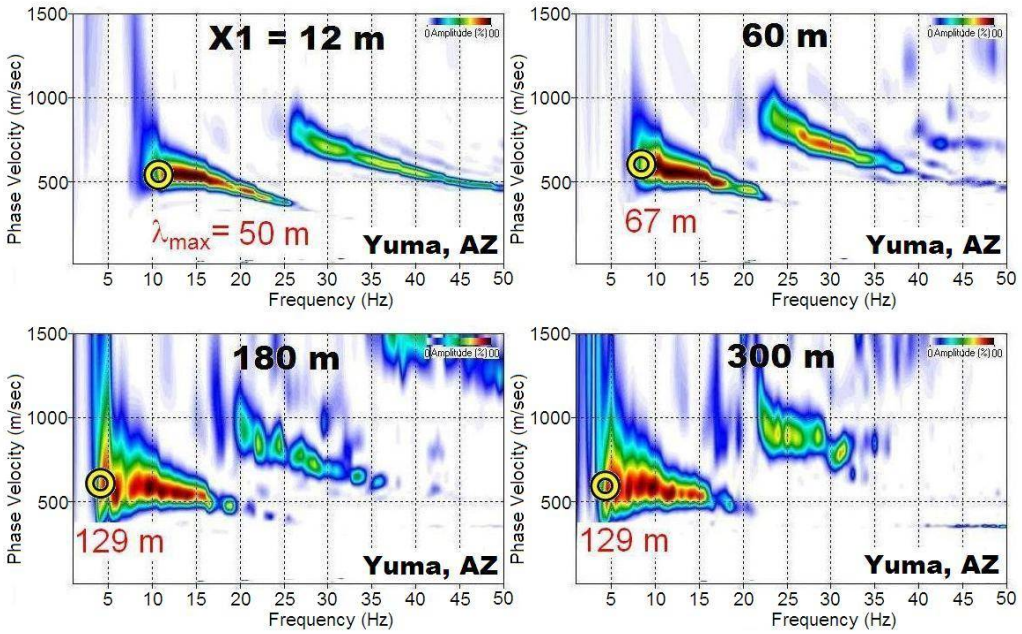

Figure 8. Dispersion images processed from SWTR field records equivalent of 120-channel recording with four different source offsets (X1's). Maximum wavelength (λmax) analyzable is marked on each image.

sponding wavelength (λmax). It is shown that a progressive increase in X1 results in a progressive lowering (increasing) of lowest frequency (maximum wavelength), which can lead to progressively deeper investigation depths (Zmax). It seems the lowest frequency has already reached the natural frequency of the geophone (4.5 Hz) when X1 was 180 m and therefore the next longer source offset of X1 = 300 m did not make any further noticeable change in the recorded surface wave energy.

DISCUSSIONS

Although study of the source offset (X1) and receiver spread length (L) has been performed in this paper with field data sets from three different sites, it needs further investigation with data sets from more diverse areas to more rigoriously scrutinize the assertions we make. In particular, it seems there can be other factor(s) involved in those oscillating features of dispersion curves sometimes occurring even at $\lambda \leq L$. Possible ways to minimize the oscillation feature is under study. Recent study by Yoon and Rix (2009) also reported similar oscillating behavior of dispersion cuves extracted from f-k transformation of synthetic and laboratory data sets without discussing possibility of influence from the transformation itself.

CONCLUSIONS

The maximum wavelength (λmax) that can be analyzed with the highest accuracy possible seems equal to about one receiver spread length (L); $\lambda max \approx L$. Attempts to analyze longer wavelengths inevitably run the risk of fluctuating inaccuracy that can be within five percent for $\lambda \leq 2L$. A large source offset (e.g., $X1 \geq L$) enhances energy for longer wavelength surface waves and increases λmax with a given receiver spread. On the other hand, a small source offset (e.g., $X1 \leq L$) cannot

only reduce λmax but also result in underestimated phase velocities. The degree of the underestimation, however, seems highly site dependent and is sometimes negligible.

ACKNOWLEDGEMENTS

We would like to acknowledge the Kansas Geological Survey (KGS) for the field data sets from SWTR and Blue Canyon Wind Farm projects used for this study. In addition, we thank Barr Engineering Company for the Wind Farm data set.

REFERENCES

Gucunski, N. and Woods, R.D. (1991). Instrumentation for SASW testing, *in* Bhatia, S.K., and Blaney, G.W., eds., Recent Advances in Instrumentation, Data Acquisition and Testing in Soil Dynamics: Am. Soc. Civil Eng., 1–16.

Miller, R.D., Anderson, T.S., Ivanov, J., Davis, J.C., Olea, R., Park, C.B., Steeples, D.W., Moran, M.L., and Xia, J. (2003). 3-D characterization of seismic properties at the Smart Weapons Test Range, YPG [Exp. Abs.]: Soc. Expl. Geophys., NSG 2.3.

Oppenheim, A. and Schafer, R.W. (1989). Discrete-time signal processing: Prentice Hall, Englewood Cliffs, New Jersey, 879 pp.

Park, C.B. and Shawver, J.B. (2009). MASW survey using multiple source offsets: Proceedings of the Symposium on the Application of Geophysics to Engineering and Environmental Problems, Fort Worth, Texas, March 29-April 2, 2009.

Park, C.B. and R.D. Miller. (2005a). Multichannel analysis of passive surface waves–modeling and processing schemes: Proceedings of the Geo-Frontiers conference, Austin, Texas, January 23-26.

Park, C.B. and Miller, R.D. (2005b). Seismic characterization of wind turbine sites near Lawton, Oklahoma, by the MASW method: Kansas Geological Survey Open-file Report 2005-22.

Park, C.B., Miller, R.D., and Xia, J. (1999). Multi-channel analysis of surface waves: Geophysics, 64 (3): 800-808.

Park, C.B., Miller, R.D., and Xia, J. (1998). Imaging dispersion curves of surface waves **o**n multi-channel record: [Exp. Abs.]: Soc. Explor. Geophys.: 1377-1380.

Richart, F.E., Hall, J.R., and Woods, R.D. (1970). Vibrations of Soils and Foundations: Prentice-Hall, Inc.

Rix, G.J. and Leipski, E.A. (1991). Accuracy and resolution of surface wave inversion, *in* Bhatia, S.K., and Blaney, G.W., eds., Recent Advances in Instrumentation, Data Acquisition and Testing in Soil Dynamics: Am. Soc. Civil Eng., 17–32.

Ryden, N. and Mooney, M. (2009). Analysis of surface waves from the light weight deflectometer: Soil Dynamics and Earthquake Engineering, 29: 1134-1142.

Stokoe II, K.H., Wright, S.G., Bay, J.A., and Roësset, J.M. (1994). Characterization of geotechnical sites by SASW method, *in* Woods, R.D., ed., Geophysical Characterization of Sites: Oxford Publishers.

Yoon, S. and Rix, G.J. (2009). Near-field effects on array-based surface wave methods with active sources: J. Geotech. Geoenviron. Eng., 135(3), 399-406.

Zhang, S.X., Chan, L.S., and Xia, J. (2004). The selection of field acquisition parameters for dispersion images from multichannel surface wave data: Pure and Applied Geophysics, 161: 1–17.